Chapter 5

Secondary deformations in nonlinear elasticity

In Section 3.2.2, we have shown that in the incompressible case, the general antiplane shear (3.64) can not be always sustained unless the axisymetric case is considered. This means that when the geometry of the material deformed moves away from axial symmetry, we can describe the deformation only for special particular materials. For example, consider the case of an elastic material filling the annular region between two coaxial cylinders, with the following boundary-value problem: hold fixed the outer cylinder and pull the inner cylinder by applying a tension in the axial direction. A solution to this problem, valid for every incompressible isotropic elastic solid, is obtained by assuming a priori that the deformation field is a pure axial shear. However if consider the corresponding problem for non-coaxial cylinders, thereby losing the axial symmetry, then it is clear that we cannot expect the material to deform as prescribed by a pure axial shear deformation. Knowles' result [72] tells us that now the boundary-value problem can be solved with a general anti-plane deformation (not axially symmetric) only for a subclass of incompressible isotropic elastic materials.

Moreover, in Sections 4.1 and 4.2, we have underlined how it is not always possible for a compressible material to sustain pure torsion and pure axial shear, respectively, unless some particular forms of strain energy functions are considered, because in general they might be accompanied by the radial deformation. In Section 4.4, some explanations about the dangers in forcing the compressible material to have some special behaviours were given.

Of course, these restrictions do not mean that, for a generic material, it is not possible to deform the solid as prescribed by our boundary conditions, but rather that, in general, these lead to a deformation field that is more complex for example than a pure torsion or than an anti-plane shear. Hence, we also expect secondary deformations: a clear difficult task to understand in solving boundary-value problem by appealing only to a semi-inverse procedure.

The theory of non-Newtonian fluid dynamics has generated a substantial literature about secondary flows, see for example Fosdick and Serrin [40]. In 1956, Ericksen [35] conjectured that purely rectilinear flows would be possible only in pipes of circular cross sections or cross sections made of straight lines and circles, secondary flows being necessarily present in pipes of arbitrary cross sections. In

1973, Fosdick and Serrin [40] proved a more precise version of the Ericksen's conjecture: requiring certain technical assumptions on regularity concerning the material properties, they showed that unless the material functions characterizing the fluid satisfied certain special relationships, the cross section ought to be a circle or the annular region between two concentric circles.

In solid mechanics, Fosdick and Kao [39] were the first to explore the counterpart to Ericksen's conjecture in fluids within the context of nonlinear elasticity. Denoting by $(\boldsymbol{i}_1, \boldsymbol{i}_2, \boldsymbol{i}_3)$ an orthonormal basis in rectangular Cartesian coordinates, they consider a cylindrical domain, whose generators are parallel to the axis $\boldsymbol{i}_3$, with bounded and connected cross section A having boundary

$$\partial A = \bigcup_{i=0}^{n} \partial A_i \tag{5.1}$$

consisting of $n+1$ sufficiently smooth non intersecting closed curves, where ∂A_0 is the external boundary of A which encloses all other inner boundaries ∂A_i $(i = 1, \dots, n)$. Fosdick and Kao [39] assume the displacement $\boldsymbol{u}$ to be decomposed into an axial component $w = w(X_1, X_2)$ and a cross sectional component $\boldsymbol{v} = \boldsymbol{v}(X_1, X_2)$ and consider the following boundary condition

$$w = \begin{cases} 0 \text{ on } \partial A_0 \\ w_i \text{ on } \partial A_i \quad (i = 1, \dots, n) \end{cases} \tag{5.2}$$

and $\boldsymbol{v} = \boldsymbol{0}$ on ∂A. First, they show that in general, rectilinear shear ($\boldsymbol{v} = \boldsymbol{0}$) of cylinders is not always possible, unless the cross-section is a circle or the annular region between two concentric circles. Then, they analyse the problem which includes not only an axial shear deformation but also the possibility of cross-sectional distortion. They use the *specific driving force* (applied shear) a, as small parameter and consider the following perturbation problem for uniformly infinitesimal boundary data,

$$\begin{gathered} a = \varepsilon \bar{a}, \quad w_i = \varepsilon \bar{w}_i \ (i = 1, 2, \dots, n) \\ w = \sum_{i=1}^{n} w^i \varepsilon^i, \quad \boldsymbol{v} = \sum_{i=1}^{n} \boldsymbol{v}^i \varepsilon^i, \end{gathered} \tag{5.3}$$

where $\varepsilon \ll 1$ is a real non-negative number, $\bar{a}$ and $\bar{w}_i$ $(i = 1, 2, \dots, n)$ are constant numbers independent of ε which carry, respectively, the dimensions of force per unit volume and displacement, and w^i, $\boldsymbol{v}^i$ $(i = 1, 2, \dots, n)$ are functions depending of the same arguments of w and $\boldsymbol{v}$, respectively. It follows immediately from the assumed form for the displacement field that when $\varepsilon = 0$, there is no displacement and this has to be expected as there is no driving force. Using (5.3), the balance equations and the constraint of incompressibility, Fosdick and Kao [39] find $\boldsymbol{v}^i = \boldsymbol{0}$ for $i = 1, 2, 3$ and show that $\boldsymbol{v}^4$ is necessary different from zero. Thus secondary deformations appear at only fourth order.

Another possibility of perturbation approach in order to investigate for secondary deformations is given by departure from circular symmetry. Mollica and Rajagopal [83] showed that in this last case the secondary deformations appear

at first order when the driving force is a fixed value placed without restrictions, the perturbation parameter being the departure from circularity. The deformation that they consider takes place between two infinite cylinders eccentrically placed and it can be driven by an axial pressure gradient or by the axial motion of one of the boundaries. They use the eccentricity ε which is the distance between the centers of cylinders as the perturbation parameter. In a Cartesian coordinates system (X, Y, Z), the equations for two cylinders, whose radii are R_1 and R_2, with $R_1 < R_2$, are

$$\begin{aligned} &X^2 + Y^2 = R_2^2, \\ &(X - |\overrightarrow{O_1O_2}|)^2 + Y^2 = R_1^2, \end{aligned} \tag{5.4}$$

where $|\overrightarrow{O_1O_2}|$ is the eccentricity and they let

$$\varepsilon = \frac{|\overrightarrow{O_1O_2}|}{R_1}, \tag{5.5}$$

be a dimensionless small parameter. Let (R, Θ, Z) and (r, θ, z) be cylindrical coordinates in reference and current configuration, respectively. Then they consider a deformation of the form

$$\begin{aligned} r &= R + \varepsilon v(R, \Theta) + o(\varepsilon), \\ \theta &= \Theta + \varepsilon w(R, \Theta) + o(\varepsilon), \\ z &= Z + f(R) + \varepsilon g(R, \Theta) + o(\varepsilon). \end{aligned} \tag{5.6}$$

At order zero ($\varepsilon = 0$), (5.6) is not the undeformed state (here it is therefore different from previous case (5.3)), but it is an axially symmetric deformation. For the problem under investigation, they assume that the outer cylinder is fixed while the inner cylinder translates in the axial direction by a fixed amount f_w. Thus, denoting by $\mathcal{C}_1$ and $\mathcal{C}_2$ the inner and outer cylinders, respectively, from (5.6), they set

$$\begin{aligned} &\varepsilon v(R, \Theta)|_{\mathcal{C}_1} = \varepsilon w(R, \Theta)|_{\mathcal{C}_1} = 0, \\ &\varepsilon v(R, \Theta)|_{\mathcal{C}_2} = \varepsilon w(R, \Theta)|_{\mathcal{C}_2} = 0, \\ &f(R) + \varepsilon g(R, \Theta)|_{\mathcal{C}_1} = f_w, \\ &f(R) + \varepsilon g(R, \Theta)|_{\mathcal{C}_2} = 0. \end{aligned} \tag{5.7}$$

After that, they suppose that the incompressible material is described by the following strain energy function

$$W(I_1, I_2) = \frac{\delta_1}{2b}\left\{\left[1 + \frac{b}{n}(I_1 - 3)\right]^n - 1\right\} - \frac{\delta_2}{2}\left\{I_2 - 3\right\}, \tag{5.8}$$

where δ_1, δ_2, b, n are material parameters. When $n = 1$, the model (5.8) reduces to the classical Mooney-Rivlin model (2.3), while if $\delta_2 = 0$, it reduces to the power-law model (2.16). As well, they set

$$\delta_1 > 0, \quad \delta_2 < 0, \quad 1 > n > \frac{1}{2}, \quad n > 1, \quad b > 0, \tag{5.9}$$

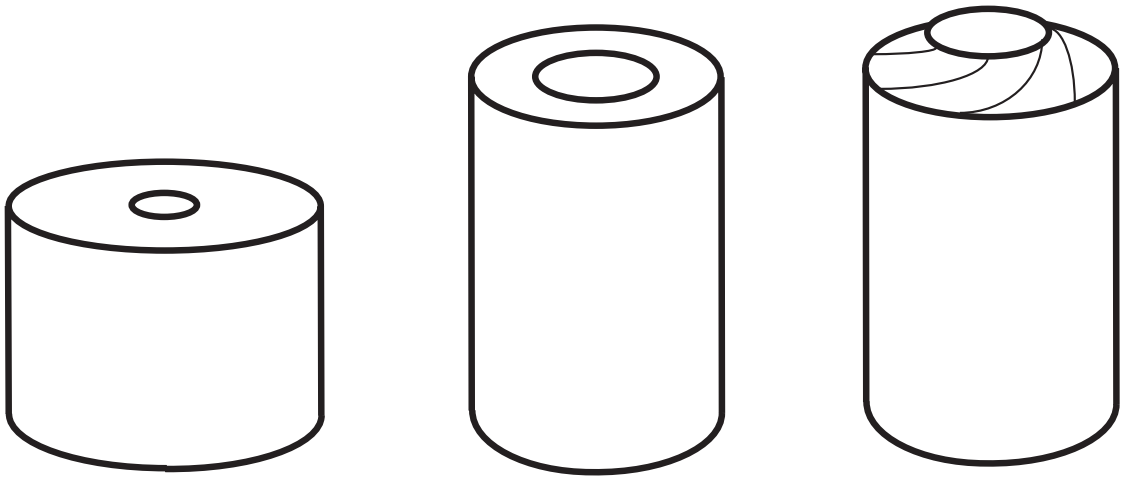

Figure 5.1: Shrink fit of an elastic tube, followed by the combination of simple torsion and helical shear. (The figure does not respect scales among the various deformations).

such that from the analysis of Fosdick and Kao [39], the material cannot exhibit a purely axial displacement when subjected to axial shear, and secondary displacements are therefore necessary. Using (5.6), the boundary conditions (5.7), the balance equations and the constraint of incompressibility, Mollica and Rajagopal [83] establish that secondary deformations at first order in ε are possible when the driving force is not small and the annular region deviates slightly from axial symmetry.

In the next section we consider a complex deformation field in isotropic incompressible elasticity, to point out by an explicit example (extracted from our work [27]) the situations just evoked, and to elaborate on their possible impact on solid mechanics. The deformation field takes advantage of the radial symmetry; therefore we find it convenient to visualize it by considering an elastic cylinder.

5.1 An analytic example of secondary deformations

For a better understanding of the "real" situation we evoke, let us imagine that a corkscrew has been driven through a cork (the cylinder) in a bottle. The inside of the bottleneck is the outer rigid cylinder and the idealization of the gallery carved out by the corkscrew constitutes the inner coaxial rigid cylinder. Our first deformation is purely radial, originated from the introduction of the cork into the bottleneck and then completed when the corkscrew penetrates the cork (a so-called *shrink fit problem*, which is a source of elastic residual stresses here). We call A, B the respective inner and outer radii of the cork in the reference configuration and $r_1 > A$, $r_2 < B$ their current counterparts. Then we follow with a simple torsion combined to a helical shear, in order to model pulling the cork out of the bottleneck in the presence of a contact force. Figure 5.1 sketches this deformation.

Of course, we are aware of the shortcomings of our modelling with respect to the

description of a "real" cork-pulling problem, because no cork is an infinitely long cylinder, nor is a corkscrew perfectly straight. In addition, traditional corks made from bark are anisotropic (honeycomb-shaped mesoscopic structure) and possess the remarkable (and little-known) property of having an infinitesimal Poisson ratio equal to zero, see the review article by Gibson *et al.* [46]. However we note that *polymer corks* have appeared on the world wine market; they are made of elastomers, for which incompressible, isotropic elasticity seems like a reasonable framework (indeed the documentation of these synthetic wine stoppers indicates that they lengthen during the sealing process)[1].

5.1.1 Equilibrium equations

Consider a long hollow cylindrical tube composed of an isotropic incompressible nonlinearly elastic material. At rest, the tube is in the region

$$A \le R \le B, \qquad 0 \le \Theta \le 2\pi, \qquad -\infty \le Z \le \infty, \tag{5.10}$$

where (R, Θ, Z) are the cylindrical coordinates associated with the undeformed configuration, and A and B are the inner and outer radii of the tube, respectively.

Consider the general deformation obtained by the combination of radial dilatation, helical shear and torsion as

$$r = r(R), \qquad \theta = \Theta + g(R) + \tau Z, \qquad z = \lambda Z + w(R), \tag{5.11}$$

where (r, θ, z) are the cylindrical coordinates in the deformed configuration; τ is the amount of torsion; and λ is the stretch ratio in the Z-direction. Here, g and w are yet unknown functions of R only. (The classical case of torsion deformation (4.1) corresponds to $w = g = 0,\ \lambda = 1$.) Hidden inside (5.11) is the *shrink fit deformation*

$$r = r(R), \qquad \theta = \Theta, \qquad z = \lambda Z, \tag{5.12}$$

which is (5.11) without any torsion or helical shear ($\tau = g = w \equiv 0$). The physical components of the deformation gradient $\boldsymbol{F}$ and of its inverse $\boldsymbol{F}^{-1}$ are then

$$\begin{bmatrix} r' & 0 & 0 \\ rg' & r/R & r\tau \\ w' & 0 & \lambda \end{bmatrix} \quad \text{and} \quad \begin{bmatrix} r\lambda/R & 0 & 0 \\ rw'\tau - rg'\lambda & r'\lambda & -rr'\tau \\ -rw'/R & 0 & rr'/R \end{bmatrix}, \tag{5.13}$$

respectively. Note that we used the incompressibility constraint in order to compute $\boldsymbol{F}^{-1}$; it states that $\det \boldsymbol{F} = 1$, so that

$$r' = \frac{R}{\lambda r}. \tag{5.14}$$

In our first deformation, the cylindrical tube is pressed into a cylindrical cavity with inner radius $r_1 > A$ and outer radius $r_2 < B$. It follows by integration of the equation (5.14) that

$$r(R) = \sqrt{\frac{R^2}{\lambda} + \alpha}, \tag{5.15}$$

[1]We hope that this study provides a first step toward a nonlinear alternative to the linear elasticity testing protocols presented in the international standard ISO 9727. We also note that low-cost *shock absorbers* often consist of a moving metal cylinder, glued to the inner face of an elastomeric tube, whose outer face is glued to a fixed metal cylinder [56].

where now

$$\alpha = \frac{B^2 r_1^2 - A^2 r_2^2}{B^2 - A^2}, \qquad \lambda = \frac{B^2 - A^2}{r_2^2 - r_1^2}. \tag{5.16}$$

We compute the physical components of the left Cauchy-Green strain tensor $\boldsymbol{B} = \boldsymbol{F}\boldsymbol{F}^T$ from (5.13) and find its first three principal invariants as

$$\begin{aligned} I_1 &= (r')^2 + (rg')^2 + (r/R)^2 + (r\tau)^2 + \lambda^2 + (w')^2, \\ I_2 &= (r\lambda/R)^2 + (rw'\tau - rg'\lambda)^2 + (rw'/R)^2 + (R/r)^2 + (1/\lambda)^2 + (R\tau/\lambda)^2, \end{aligned} \tag{5.17}$$

and of course, $I_3 = 1$. For a general incompressible hyperelastic solid, the Cauchy stress tensor $\boldsymbol{T}$ is given by (1.40). Having computed $\boldsymbol{B}^{-1} = (\boldsymbol{F}^T)^{-1}\boldsymbol{F}^{-1}$ from (5.13), we find that the components of $\boldsymbol{T}$ are

$$\begin{aligned} T_{rr} &= -p + 2W_1(r')^2 - 2W_2\left[(r\lambda/R)^2 + (rw'\tau - rg'\lambda)^2 + (rw'/R)^2\right], \\ T_{\theta\theta} &= -p + 2W_1\left[(rg')^2 + (r/R)^2 + (r\tau)^2\right] - 2W_2(R/r)^2, \\ T_{zz} &= -p + 2W_1[\lambda^2 + (w')^2] - 2W_2\left[(1/\lambda)^2 + (R\tau/\lambda)^2\right], \\ T_{r\theta} &= 2W_1(rr'g') - 2W_2(w'\tau - g'\lambda)R, \\ T_{rz} &= 2W_1(r'w') - 2W_2\left[rRg'\tau - rRw'\tau^2/\lambda - rw'/(\lambda R)\right], \\ T_{\theta z} &= 2W_1(rw'g' + r\lambda\tau) + 2W_2(r'R\tau). \end{aligned} \tag{5.18}$$

Finally the equilibrium equations, in the absence of body forces, are: div $\boldsymbol{T} = \boldsymbol{0}$; for fields depending only on the radial coordinate as shown here, they reduce to

$$\begin{aligned} &\frac{\mathrm{d}T_{rr}}{\mathrm{d}r} + \frac{T_{rr} - T_{\theta\theta}}{r} = 0, \\ &\frac{\mathrm{d}T_{r\theta}}{\mathrm{d}r} + \frac{2}{r}T_{r\theta} = 0, \\ &\frac{\mathrm{d}T_{rz}}{\mathrm{d}r} + \frac{1}{r}T_{rz} = 0. \end{aligned} \tag{5.19}$$

5.1.2 Boundary conditions

Now consider the inner face of the tube: we assume that it is subject to a vertical pull,

$$T_{rz}(A) = T_0^A, \qquad T_{r\theta}(A) = 0, \tag{5.20}$$

say. Then by integrating the second and third equations of equilibrium $(5.19)_{2,3}$, we find that

$$T_{rz}(r) = \frac{r_1}{r}T_0^A, \qquad T_{r\theta}(r) = 0. \tag{5.21}$$

The outer face of the tube (in contact with the glass in the cork/bottle problem) remains fixed, so that

$$w(B) = 0, \qquad g(B) = 0, \qquad T_{rr}(B) = T_0, \tag{5.22}$$

say. In addition to the axial traction applied on its inner face, the tube is subject to a resultant axial force N (say) and a resultant moment M (say),

$$N = \int_0^{2\pi}\int_{r_1}^{r_2} T_{zz} r \mathrm{d}r\mathrm{d}\theta, \qquad M = \int_0^{2\pi}\int_{r_1}^{r_2} T_{\theta z} r^2 \mathrm{d}r\mathrm{d}\theta. \tag{5.23}$$

Note that the traction T_0 of (5.22) is not arbitrary but is instead determined by the *shrink fit pre-deformation* (5.12), by requiring that $N = 0$ when $T_0^A = \tau = g = w \equiv 0$ (this process is detailed in the Section 5.1.3 for the neo-Hookean material). Therefore, T_0 is connected with the stress field experienced by the cork when it is introduced in the bottleneck. In the rest of this explanation we aim at presenting results in dimensionless form. To this end, we normalize the strain energy function W and the Cauchy stress tensor $\boldsymbol{T}$ with respect to μ, the infinitesimal shear modulus; hence we introduce $\overline{W}$ and $\overline{\boldsymbol{T}}$ defined by

$$\overline{W} = \frac{W}{\mu}, \qquad \overline{\boldsymbol{T}} = \frac{\boldsymbol{T}}{\mu}. \tag{5.24}$$

Similarly we introduce the following non-dimensional variables,

$$\eta = \frac{A}{B}, \quad \overline{R} = \frac{R}{B}, \quad \overline{r}_i = \frac{r_i}{B}, \quad \overline{w} = \frac{w}{B}, \quad \overline{\alpha} = \frac{\alpha}{B^2}, \quad \overline{\tau} = B\tau, \tag{5.25}$$

so that $\eta \leq \overline{R} \leq 1$. Also, we find from (5.16) that

$$\overline{\alpha} = \frac{\overline{r}_1^2 - \eta^2 \overline{r}_2^2}{1 - \eta^2}, \qquad \lambda = \frac{1 - \eta^2}{\overline{r}_2^2 - \overline{r}_1^2}. \tag{5.26}$$

Turning to our cork or shock absorber problems, we imagine that the inner metal cylinder is introduced into a pre-existing cylindrical cavity (this precaution ensures a one-to-one correspondence of the material points between the reference and the current configurations). In our upcoming numerical simulations, we take $A = B/10$ so that $\eta = 0.1$; we consider that the outer radius is shrunk by 10%, $r_2 = 0.9B$, and that the inner radius is doubled, $r_1 = 2A$; finally, we apply a traction, the magnitude of which is half the infinitesimal shear modulus: $|T_0^A| = \mu/2$. This gives

$$\overline{\alpha} \simeq 3.22 \times 10^{-2}, \qquad \lambda \simeq 1.286, \qquad \overline{T}_0^A = -0.5. \tag{5.27}$$

At this point it is possible to state clearly our main observation. A first glance at the boundary conditions, in particular at the requirements that g be zero on the outer face of the tube, gives the expectation that $g \equiv 0$ everywhere is a solution to our boundary-value problem, at least for some simple forms of the constitutive equations. In what follows, we find that, for the neo-Hookean solids, $g \equiv 0$ is indeed a solution, whether there is a torsion τ or not. However if the solid is not neo-Hookean, then it is necessary that $g \neq 0$ when $\tau \neq 0$, and the picture becomes more complex. For this reason, we classify as "purely academic" the question:

> *Which is the most general strain-energy density for which it is possible to solve the above boundary value problem with $g \equiv 0$?*

Indeed, there is no "real world" material, the behaviour of which is ever going to be described *exactly* by that strain-energy density (supposing it exists). Instead a more pertinent issue to raise for "real word applications" is whether we are able to evaluate the importance of latent (secondary) stress fields, because they are bound to be woken up (triggered) by the deformation.

5.1.3 neo-Hookean materials

First, we consider the special strain energy function which generates the class of neo-Hookean materials (2.1). Note that here and hereafter, we use the non-dimensional quantities introduced previously, from which we drop the overbar for convenience. Hence, the components of the (non-dimensional) stress field in a neo-Hookean material reduce to

$$\begin{aligned} &T_{rr} = -p + (r')^2, && T_{\theta\theta} = -p + (rg')^2 + (r/R)^2 + (r\tau)^2, \\ &T_{zz} = -p + \lambda^2 + (w')^2, && T_{r\theta} = rr'g', \\ &T_{rz} = r'w', && T_{\theta z} = rg'w' + r\lambda\tau. \end{aligned} \tag{5.28}$$

Substituting into (5.21) we find that

$$w' = \lambda r_1 T_0^A / R, \qquad g' = 0, \tag{5.29}$$

and by integration, using (5.22), that

$$w = \lambda r_1 T_0^A \ln R, \qquad g = 0. \tag{5.30}$$

In Figure 5.2a, we present a rectangle in the tube at rest, which is delimited by $0.1 \leq R \leq 1.0$ and $0.0 \leq Z \leq 1.0$. Then it is subject to the deformation corresponding to the numerical values of (5.27). To generate Figure 5.2b, we computed the resulting shape for a neo-Hookean tube, using (5.11), (5.15), and (5.30).

Now that we know the full deformation field, (see (5.11) and (5.30)), we can compute $T_{rr} - T_{\theta\theta}$ from (5.28) and deduce T_{rr} by integration of $(5.19)_1$, with initial condition $(5.22)_3$. Then the other field quantities follow from the rest of (5.28). Finally, we find in turn that

$$\begin{aligned} T_{rr} &= \frac{1}{2\lambda}\left\{\ln\frac{\lambda r_2^2 R^2}{R^2+\alpha\lambda} + (R^2-1)\left[\frac{\alpha}{r_2^2\,(R^2+\alpha\lambda)} + \tau^2\right]\right\} + T_0, \\ T_{\theta\theta} &= T_{rr} + \left(\frac{R^2}{\lambda}+\alpha\right)\left(\frac{1}{R^2}+\tau^2\right) - \frac{R^2}{\lambda(R^2+\alpha\lambda)}, \\ T_{zz} &= T_{rr} + \lambda^2\left(1 + \frac{r_1^2 (T_0^A)^2}{R^2}\right) - \frac{R^2}{\lambda(R^2+\alpha\lambda)} \end{aligned} \tag{5.31}$$

(where we used the identity $1 + \alpha\lambda = \lambda r_2^2$, see (5.15) with $R = 1$), and that

$$T_{r\theta} = 0, \qquad T_{rz} = \frac{r_1}{\sqrt{\dfrac{R^2}{\lambda}+\alpha}} T_0^A, \qquad T_{\theta z} = \lambda\tau\sqrt{\frac{R^2}{\lambda}+\alpha}. \tag{5.32}$$

The constant T_0 is fixed by the shrink fit pre-deformation (5.12), imposing that $N = 0$ when $\tau = g = w = T_0^A \equiv 0$, or

$$(T_0+\lambda^2)(1-\eta^2) + \frac{1}{\lambda}\int_\eta^1 \left[\ln\frac{\lambda r_2^2 R^2}{R^2+\alpha\lambda} + \frac{\alpha(R^2-1)}{r_2^2(R^2+\alpha\lambda)} - \frac{2R^2}{R^2+\alpha\lambda}\right] R\mathrm{d}R = 0. \tag{5.33}$$

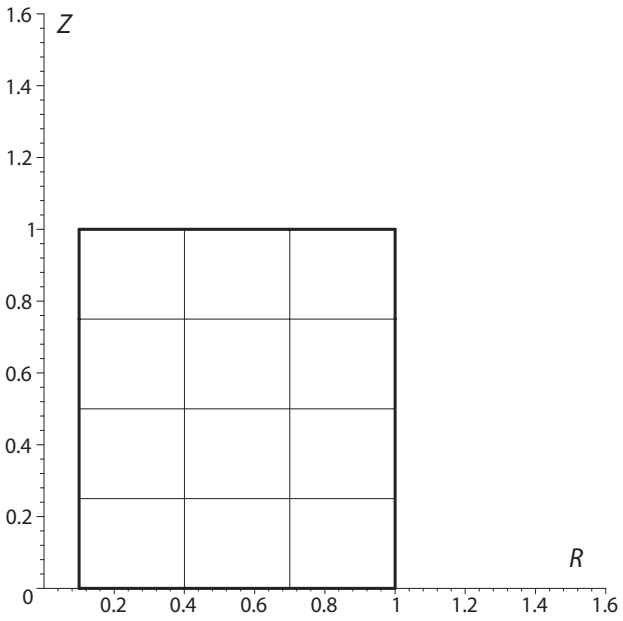

(a)

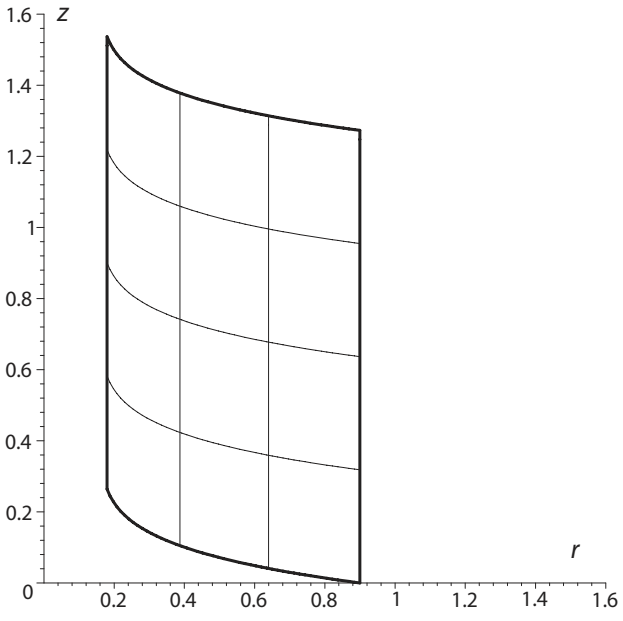

(b)

Figure 5.2: (a, b) Pulling on the inside face of a neo-Hookean tube. Here the vertical axis is the symmetry axis of the tube.

Using (5.33) and (5.23), (5.31), (5.32), we find the following expressions for the resultant moment,

$$M = \pi(r_2^4 - r_1^4)\lambda\tau/2, \tag{5.34}$$

and for the axial force,

$$N = 2\pi\lambda r_1^2 |\ln\eta| \left(T_0^A\right)^2 - \frac{\pi}{4}(r_2^2 - r_1^2)^2\tau^2. \tag{5.35}$$

We now have a clear picture of the response of a neo-Hookean solid to the deformation (5.11), with the boundary conditions of Section 5.1.2. First, we saw that here the contribution $g(R)$ is not required for the azimuthal displacement, whether there is a torsion τ or not. Also, if a moment $M \neq 0$ is applied, then the tube suffers an amount of torsion $\tau \neq 0$ proportional to M. On the other hand, if the tube is pulled by the application of an axial force only ($N \neq 0$) and no moment ($M = 0$), then $\tau = 0$ and no azimuthal shear occurs at all.

5.1.4 Generalized neo-Hookean materials

As a first broadening of the neo-Hookean strain-energy density (2.1), we consider generalized neo-Hookean materials (2.12). To gain access to the Cauchy stress components in this context, it suffices to take $W_2 = 0$ and $W_1 = W'$, where the prime stands for the derivatives of W with respect to the first invariant, in equations (5.18). In particular,

$$T_{r\theta} = 2rr'g'W', \tag{5.36}$$

and the integrated equation of equilibrium $(5.21)_2$ gives $g' = 0$. By integrating, with $(5.22)_2$ as an initial value, we find that

$$g \equiv 0. \tag{5.37}$$

Hence, just as in the neo-Hookean case, azimuthal shear can be avoided altogether, whether there is a torsion τ or not. We are left with an equation for the axial shear, namely $(5.21)_1$, which can be written as

$$2W'(I_1)w'(R) = \frac{\lambda r_1}{R}T_0^A. \tag{5.38}$$

Obviously the same steps as those taken for neo-Hookean solids may be followed here for any given strain energy density (2.12), but now by resorting to a numerical treatment. Horgan and Saccomandi [62] show, through some specific examples of hardening generalized neo-Hookean solids, how rapidly involved the analysis becomes, even when there is only helical shear and no shrink fit. Instead, we simply point out some striking differences between our present situation and the neo-Hookean case. We remark that I_1 is of the form $(5.17)_1$ at $g \equiv 0$, i.e.

$$I_1 = \lambda^2 + \frac{R^2}{\lambda(R^2 + \alpha\lambda)} + \left(\frac{R^2}{\lambda} + \alpha\right)\left(\frac{1}{R^2} + \tau^2\right) + [w'(R)]^2. \tag{5.39}$$

It follows that (5.38) is a nonlinear differential equation for w', in contrast to the neo-Hookean case. Another contrast is that the axial shear w is now intimately

coupled to the torsion parameter τ, and that this dependence is a *second-order effect* (τ appears above as τ^2).

A similar problem where the azimuthal shear has not been ignored, but the axial shear has been considered null, i.e. $w \equiv 0$ has been recently considered by Wineman [130].

5.1.5 Mooney–Rivlin materials

In this section, we specialize the general equations of section 5.1.1 to the Mooney–Rivlin form of the strain energy function (2.3), which in its non-dimensional form reads

$$W = \frac{I_1 - 3 + m(I_2 - 3)}{2(1+m)}, \tag{5.40}$$

so that

$$2W_1 = \frac{1}{1+m}, \qquad 2W_2 = \frac{m}{1+m}, \tag{5.41}$$

where $m > 0$ is a material parameter, distinguishing the Mooney–Rivlin material from the neo-Hookean material (2.1), and also allowing a dependence on the second principal strain invariant I_2, in contrast to the generalized neo-Hookean solids of the previous section. Then the integrated equations of equilibrium (5.21) read

$$\begin{aligned} &\left(R + m\tau^2 r^2 R + mr^2/R\right) w' - (m\tau\lambda r^2 R) g' = (1+m)\lambda r_1 T_0^A, \\ &(m\tau\lambda) w' - (1 + m\lambda^2) g' = 0. \end{aligned} \tag{5.42}$$

First we ask ourselves if it is possible to avoid torsion during the pulling of the inner face. Taking $\tau = 0$ above gives

$$(R + mr^2/R) w' = (1+m)\lambda r_1 T_0^A, \qquad g' = 0. \tag{5.43}$$

It follows that here it is indeed possible to solve our boundary value problem. We find

$$w = \lambda r_1 T_0^A \, \frac{\lambda(1+m)}{2(\lambda+m)} \ln\left[\frac{m\alpha\lambda + (\lambda+m)R^2}{m\alpha\lambda + (\lambda+m)}\right], \qquad g = 0. \tag{5.44}$$

However if $\tau \neq 0$, then it is necessary that $g \neq 0$, otherwise $(5.42)_2$ gives $w' = 0$ while $(5.42)_1$ gives $w' \neq 0$, a contradiction. This constitutes the first departure from the neo-Hookean and generalized neo-Hookean behaviours: *torsion ($\tau \neq 0$) is necessarily accompanied by azimuthal shear ($g \neq 0$).* In the case $\tau \neq 0$, we introduce the function $\Lambda = \Lambda(R)$ defined as

$$\Lambda(R) = (R + mr^2/R)(1 + m\lambda^2) + m\tau^2 r^2 R, \tag{5.45}$$

(recall that $r = r(R)$ is given explicitly in (5.15)). We then solve the system (5.42) for w' and g' as

$$w' = (1+m)(1+m\lambda^2)\lambda \frac{T_0^A}{\Lambda(R)} r_1, \qquad g' = m(1+m)\lambda^2 \frac{T_0^A}{\Lambda(R)} \tau r_1, \tag{5.46}$$

making clear the link between g and τ. Thus for the Mooney–Rivlin material, the azimuthal shear g is a *latent* mode of deformation; it is *woken up* by any

amount of torsion τ. Recall that, at first sight, the azimuthal shear component of the deformation (5.11) seemed inessential to satisfy the boundary conditions, especially in view of the boundary condition $g(1) = 0$. However, a non-zero W_2 term in the constitutive equation clearly couples the effects of a torsion and an azimuthal shear, as displayed explicitly by the presence of τ in the expression for g' above. It is perfectly possible to integrate equations (5.46) in the general case, but to save space we do not reproduce the resulting long expressions. With them, we generated the deformation field picture of Figure 5.3(a,b) and Figure 5.4(a,b). There we took the numerical values of (5.27) for α, λ, T_0^A; we took a Mooney–Rivlin solid with $m = 5.0$; we imposed a torsion of amount $\tau = 0.5$; and we looked at the deformation field in the plane $Z = 1$ (reference configuration) and $z = \lambda$ (current configuration).

Although the secondary fields appear to be slight in the picture, they are nonetheless truly present and cannot be neglected. To show this, we consider a perturbation method to obtain simpler solutions and to understand the effect of the coupling, by taking m small. Then integrating (5.46), we find at first order that

$$\begin{aligned}
\frac{w}{r_1 T_0^A} &\simeq (1+m)\lambda \ln R - \frac{1}{2} m \left[\tau^2 R^2 + 2(1+\tau^2\alpha\lambda)\ln R - \alpha\lambda/R^2 - \tau^2 + \alpha\lambda\right], \\
\frac{g}{r_1 T_0^A} &\simeq \lambda^2 \tau m \ln R.
\end{aligned} \tag{5.47}$$

Hence, the secondary field g exists even for a nearly neo-Hookean solid (if m is small, then g is of order m.) Interestingly, we also note that the azimuthal shear g in (5.47) varies in a homogeneous and linear manner with respect to the torsion parameter τ and in a quadratic manner with respect to the axial stretch λ, showing that the presence of this secondary deformation field cannot be neglected when the effects of both the prestress and the torsion are taken into account. To complete the picture, we use the first-order approximations

$$2W_1 \simeq 1 - m, \qquad 2W_2 \simeq m, \tag{5.48}$$

to obtain the stress field as

$$\begin{aligned}
T_{rr} &\simeq -p + (1-m)\,(r')^2 - m\left\{(r\lambda/R)^2 + \left[(r\tau)^2 + (r/R)^2\right]\left(\lambda r_1 T_0^A\right)^2/R^2\right\}, \\
T_{\theta\theta} &\simeq -p + (1-m)\left[(r/R)^2 + (r\tau)^2\right] - m(R/r)^2, \\
T_{zz} &\simeq -p + \left(\lambda T_0^A r_1\right)^2\left[\left(1+2m\lambda^2\right)\frac{1}{R^2} - \frac{2}{R}\left(\frac{\tau^2 r^2}{R} + \frac{r^2}{R^3} + \frac{\lambda^2}{R} - \frac{1}{2R}\right)m\right] \\
&\qquad + (1-m)\,\lambda^2 - m\left[(1/\lambda)^2 + (R\tau/\lambda)^2\right], \\
T_{r\theta} &\simeq r r' g' - m\lambda r_1 T_0^A \tau, \\
T_{rz} &\simeq (1-m)\,(r'w') + m\lambda r_1 T_0^A\left[rR\tau^2/\lambda + r/(\lambda R)\right]/R, \\
T_{\theta z} &\simeq (1-m)\,r\lambda\tau + \lambda r r_1 T_0^A g'/R + m(r' R\tau).
\end{aligned} \tag{5.49}$$

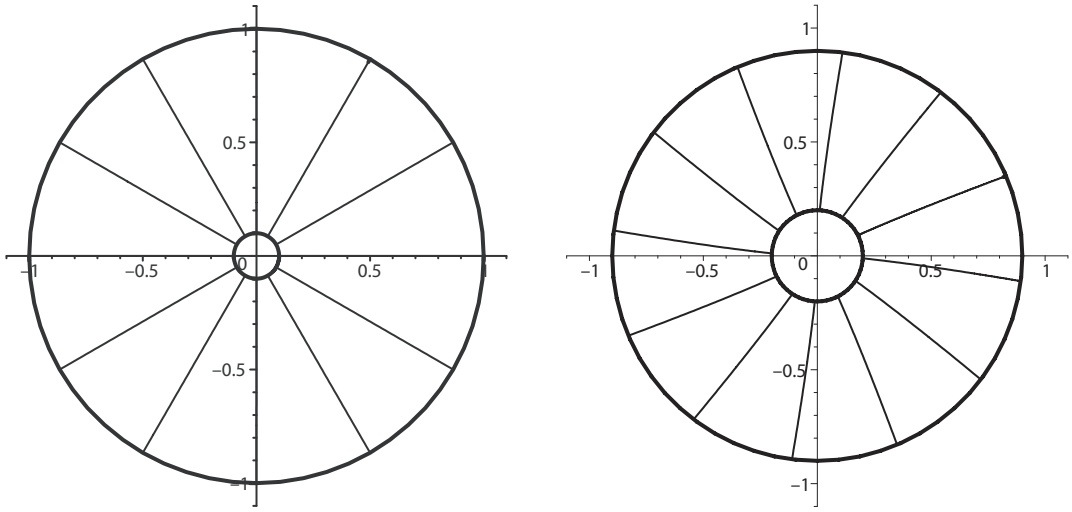

(a) (b)

Figure 5.3: (a, b) Pulling on the inside face of a Mooney–Rivlin tube, with a clockwise torsion. We have setted $m = 5.0,\ A = B/10,\ r_1 = 2A,\ r_2 = 0.9B,\ \tau = 0.5,\ |T_0^A| = \mu/2$.

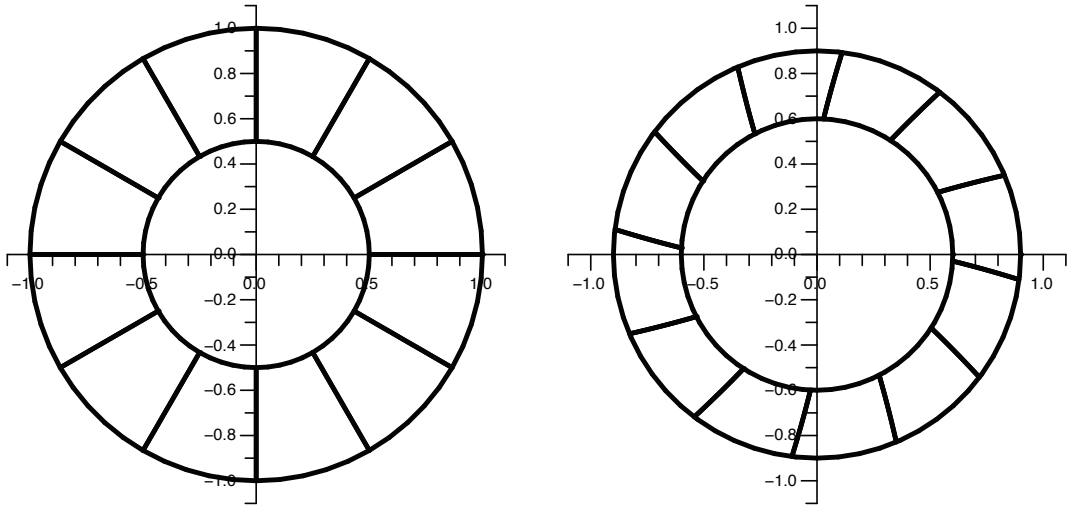

(a) (b)

Figure 5.4: (a, b) Pulling on the inside face of a Mooney–Rivlin tube, with a clockwise torsion. We have setted $m = 5.0,\ A = B/2,\ r_1 = 0.6B,\ r_2 = 0.9B,\ \tau = 0.5,\ |T_0^A| = \mu/2$.

5.2 Final remarks

In non-Newtonian fluid mechanics and in turbulence theory, the existence of shear-induced normal stresses on planes transverse to the direction of shear is at the root of some important phenomena occurring in the flow of fluid down pipes of non-circular cross section (see [40]). In other words, pure parallel flows in tubes without axial symmetry are possible only when we consider the classical theory of Navier-Stokes equations or the linear theory of turbulence or tubes of circular cross section.

In nonlinear elasticity theory, similar phenomena are reported. Hence Fosdick and Kao [39] and Mollica and Rajagopal [83] show that, for general isotropic incompressible materials, an anti-plane shear deformation of a cylinder with non axial-symmetric cross section causes a secondary in-plane deformation field, because of normal stress differences. In compressible nonlinear elasticity pure torsion is possible only in a special class of materials, but we know that torsion plus a radial displacement is possible in all compressible isotropic elastic materials.

Now a further example is given in the literature from our recent work [27], where axial symmetry holds and the boundary conditions suggest that an axial shear deformation field is sufficient to solve the boundary value problem, but nevertheless, the normal stress difference wakes up a latent azimuthal shear deformation.

> *In conclusion, from these notes, it comes out that it is not really as crucial to determine the class of materials for which a given deformation field is possible, as it may be crucial to classify all the latent deformations associated with a given deformation field in such a way that this field is controllable for the entire class of materials. Indeed, no "real" material, even when we accept that its mechanical behaviour is purely elastic, is ever going to be described exactly by a special choice of strain-energy. Looking for special classes of materials for which special deformations fields are admissible may mislead us in our understanding of the nonlinear mechanical behaviour of materials.*

5.3 A nice conjecture in solid mechanics

In the example discussed for secondary deformation, we have used a strong analogy with a cork-pulling problem, by modelling a cork as an incompressible rubber-like material. When we try to apply the previous results to the extraction of a cork from the neck of a bottle, the following remarks seem to be relevant. From the elementary theory of Coulomb friction, it is known that the pulled cork starts to move when, in modulus, the friction force exerted on the neck surface is equal to the normal force times the coefficient of static friction. In our case this means that

$$\sqrt{|T_{rz}(1)|^2 + |T_{r\theta}(1)|^2} = f_S\,|T_{rr}(1)| = f_S\,|T_0|\,, \tag{5.50}$$

where f_S is the coefficient of static friction. Using (5.21), we find that the elements of the left handside of equality (5.50) are

$$T_{rz}(1) = (r_1/r_2)T_0^A, \qquad T_{r\theta}(1) = 0. \tag{5.51}$$

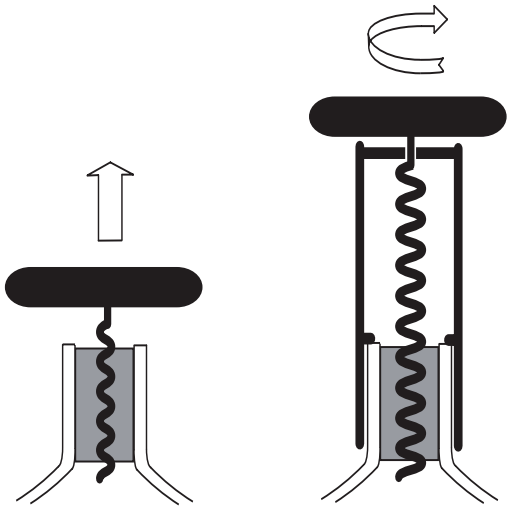

Figure 5.5: There are two main types of corkscrews: one that relies on pulling only (left) and one that adds a twist to the cork-pulling action (right). The analysis developed, indicates that the second type is more efficient.

Now, our main concern is to understand if it is better to apply a moment $M \neq 0$ when uncorking a bottle, than to pull only. First we suppose the cork is described by a neo-Hookean model (2.1). Then, to address this question, we note that the left-hand side of inequality (5.50) increases when $|T_0^A|$ increases; on the other hand, combining (5.34) and (5.35), we have

$$(T_0^A)^2 = \frac{\left[N + \frac{1}{\pi\lambda^2(r_1^2+r_2^2)^2} M^2\right]}{(2\pi\lambda r_1^2 |\ln \eta|)}. \tag{5.52}$$

It is now clear, that for a fixed value of T_0^A, in the case $M \neq 0$, it is necessary to apply an axial force, the intensity of which is less than the one in the case $M = 0$. Moreover, Equation (5.52) shows that $\left(T_0^A\right)^2$ grows linearly with N but quadratically with M^2. With respect to efficient cork-pulling, the conclusion is that adding a twisting moment to a given pure axial force is more advantageous than solely increasing the vertical pull. Moreover, we observe that a moment is applied by using a lever and this is always more convenient from an energetic point of view. Recall that we made several simplifying assumptions to reach these results: not only infinite axial length, incompressibility, and isotropy, but also the choice of a truly special strain energy function.

In the end, we evoke a classic wine party dilemma:

> *Which kind of corkscrew system requires the least effort to uncork a bottle?*

Figure 5.5 sketches the two working principles commonly found in commercial corkscrews. The most common type (on the left) relies on pulling only (directly or

[2]Using the stress field (5.49) it is straightforward, but long and cumbersome, to derive the analogue for a Mooney–Rivlin solid with a small m of relation (5.52) (which was established for neo-Hookean solids). However, nothing truly new is gained from these complex formulae with respect to the simple neo-Hookean case, and we do not pursue this aspect any further.

through levers) and the other type (on the right) relies on a combination of pulling and twisting. Notwithstanding the shortcomings of this model with respect to an actual uncorking, we are confident that we have provided a scientific argument to those wine amateurs who favour the second type of corkscrews over the first.

Notes

In this chapter we have emphasized another important aspect in the use of the semi-inverse method: the emergence of secondary flows in fluid dynamics and of latent deformations (secondary fields) in solid mechanics. Navier-Stokes fluids or isotropic incompressible hyperelastic materials are clearly constructions of the mind. No real-world fluid is exactly a Navier-Stokes fluid and no real-world elastomer can be precisely characterized from a given elastic strain energy (in fact, the experimental data associated with the extension of a rubber band can be approximated by several, widely different, strain energy functions). It is fundamental to keep this observation in mind in order to understand that the results obtained by a semi-inverse method can be misleading at times. For example, we know that a Navier-Stokes fluid can move by parallels flows in a cylindrical tube of arbitrary section. To derive this result, we use the semi-inverse method by considering that the velocity possesses a non-zero component only along the generatrix of the cylinder and that this field is a function of the section variables only; then the Navier-Stokes equations are reduced to a linear parabolic equation which we solve by taking no-slip boundary conditions. This picture is specific to Navier-Stokes fluids. In fact, if the relation between the stress and the stretching is not linear, then a fluid can flow in a tube by parallel flows if and only if the tube possesses cylindrical symmetry (see Fosdick and Serrin [40]). If the tube is not cylindrically symmetric, then what is going on? Clearly any real fluid may flow in a tube, irrespective of whether it is a Navier-Stokes fluid or not. In reality we observe the birth of secondary flows, i.e. flows in the section of the cylinder. The true, meaningful problem is to understand when these secondary flows can be or cannot be neglected; it is not to determine for which special theory secondary flows disappear.

Here, an analogous phenomenon in non-linear elasticity is derived where the counterpart to secondary flows is the notion of latent deformations, i.e. deformations that are woken up from particular boundary conditions. Boundary conditions allow semi-inverse simple solutions for special materials, but for general materials they pose very difficult tasks. Many studies (see Chapter 4) sought to characterize the special strain energy functions for which particular classes of deformations turn out to be possible (or, using a standard terminology, turn out to be controllable). For example: which elastic compressible isotropic materials support simple isochoric torsion? In fact, it is of no utility to understand which materials possess this property, because these materials do not exist. It is far more important to understand which complex geometrical deformation accompanies the action of a moment twisting a cylinder. The range of results to be derived possesses meaningful applications, most importantly in biomechanics. In hemo-dynamics, it is often assumed that the arterial wall deforms according to simple geometric fields, but this hypothesis does not take into account several fundamental factors. A specific

example is the effect of torsion on microvenous anastomotic patency and early thrombolytic phenomenon (see Selvaggi et al. [116]).

While there exists a remarkable literature on secondary flows in fluid dynamics, most notably by Rivlin, Ericksen, and Green (see for example the classic paper [109]), very little is known in solid mechanics about latent deformations. The main references in that area are: Fosdick and Kao [39], Mollica and Rajagopal [83], Horgan and Saccomandi [63].

Of course, our work [27] is another result to add to the previous ones, enriching therefore the literature of latent deformations in solid mechanics. The article [27] has been noticed in Science magazine [31/08/07, 317, no 5842, 1151, DOI: 10.1126/science.317.5842.1151a] where the paper has been qualified

A very nice application of the theory of nonlinear elasticity,

and noticed also by the Daily Telegraph [22/08/07] and La Recherche [11/07].